

Harmonic Reduction Methods at DC Side of Parallel-Connected Multipulse Rectifiers: A Review

Qingxiao Du , Lei Gao , Quanhui Li, Taiqi Li, and Fangang Meng , *Member, IEEE*

Abstract—This article gives a detailed literature review of harmonic reduction methods at the dc side of parallel-connected multipulse rectifiers (MPRs). First, passive and active harmonic reduction mechanisms are derived. Then, some commonly used and novel dc-side passive, active, and hybrid harmonic reduction circuits are discussed in terms of their structures, operation principles, and harmonic elimination performances mainly reflected on input current total harmonic distortion (THD) values. Comparisons of their design complexity, reliability, adaptability, and other aspects are also considered. Finally, simulation results are presented to verify the effectiveness of the reviewed dc-side harmonic reduction methods. This article can provide a guideline for selecting or designing rectifiers with reduced dc-side harmonics for specific applications. Anticipated trends in MPRs with lower harmonic content are also summarized.

Index Terms—Choose or design guideline, dc-side harmonic reduction mechanism, harmonic reduction method, parallel-connected multipulse rectifier (MPR), power quality improvement.

I. INTRODUCTION

THE multipulse rectifiers (MPRs) have properties of high reliability, remarkable harmonic reduction effect, and good electromagnetic compatibility so that they are widely used in industrial fields, such as the adjustable speed drive system, high-voltage direct current transmission, uninterruptable power system, large capacity magnet power supply, and aircraft converter system [1], [2]. In these occasions, the MPR serves as the interface between the ac power grid and the electric equipment, whose input and output power quality respectively determines whether the power grid and equipment can operate normally. Therefore, how to reduce the harmonic pollution caused by the time-varying and nonlinear of rectifiers has become important and meaningful research.

Generally, the harmonic reduction ability of MPRs improves as increasing of pulse number. In order to obtain a higher pulse number, two kinds of methods are proposed in previous research works. One method is to increase the output phase

number of the phase-shifting transformer [1], [3]–[5]; the other method is combines dc-side harmonic reduction methods with conventional MPRs [6]–[40]. The key point of the first method is to correctly design the winding configuration of the transformer, which has an essential impact on rectifiers' harmonic reduction performances. For the parallel-connected MPR, the second method is often applied to a conventional 12-pulse rectifier with simple structure and inherent harmonic reduction ability, which only contains two sets of three-phase bridge rectifiers and totally eliminates the fifth and seventh harmonics. Although dc-side harmonic reduction methods may achieve better effects in combination with the 18-pulse rectifier, 24-pulse rectifier, or other conventional MPRs [41]–[43], the increase of the three-phase rectifier bridges increases the complexity and cost of the whole rectification system. To achieve a better tradeoff between harmonic reduction performances and other aspects, some related research works are concentrated on a parallel-connected 12-pulse rectifier. After using the dc-side harmonic reduction methods, the high-content 11th and 13th harmonics remarkably decrease to the desired level, which satisfies power quality requirements in most industrial applications.

There are some literature reviews that concentrated on power quality improvement methods of ac–dc converters [1], [2], [44], [45], but since emphasis points are different, effective dc-side passive or active harmonic reduction methods for MPRs have not been comprehensively summarized in available reviews. Reviews of single-phase and three-phase ac–dc converters with improved power quality were respectively published by Prof. B. Singh *et al.* [44] and [45]. Based on previous research works, a review of multipulse ac–dc converters with improving power quality was proposed in [1]. In [1], multipulse ac–dc converters are categorized based on their pulse numbers, the main method introduced for increasing pulse number of MPRs is an increasing number of bridge rectifiers or diodes (thyristors) connected with the output side of the phase-shifting transformer. This method has a certain harmonic reduction ability, but complex and bulky phase-shifting transformer is often needed to acquire more output phases. With further study of MPRs, previous passive or active methods for pulse number increases are not identified as an optimum choice at present; more and more research works are focused on dc-side harmonic reduction methods based on a conventional 12-pulse parallel-connected rectifier. Another review about multipulse ac–dc converters was published in [2] that uses three tables and very concise texts to show the classifications of converters and harmonic reduction methods, but only 48-pulse rectifier with the dc-side four-tapped interphase reactor (IPR)

Manuscript received January 2, 2020; revised June 22, 2020; accepted July 27, 2020. Date of publication August 3, 2020; date of current version October 30, 2020. This work was supported by the National Natural Foundation of China under Grant 51777042. Recommended for publication by Associate Editor L. Zhang. (*Corresponding author: Fangang Meng.*)

The authors are with the School of Electrical Engineering and Automation, Harbin Institute of Technology, Harbin 150001, China (e-mail: 690384469@qq.com; hualeier111@126.com; a875921420@qq.com; 1357920795@qq.com; mfg0327@sina.com).

Color versions of one or more of the figures in this article are available online at <https://ieeexplore.ieee.org>.

Digital Object Identifier 10.1109/TPEL.2020.3013407

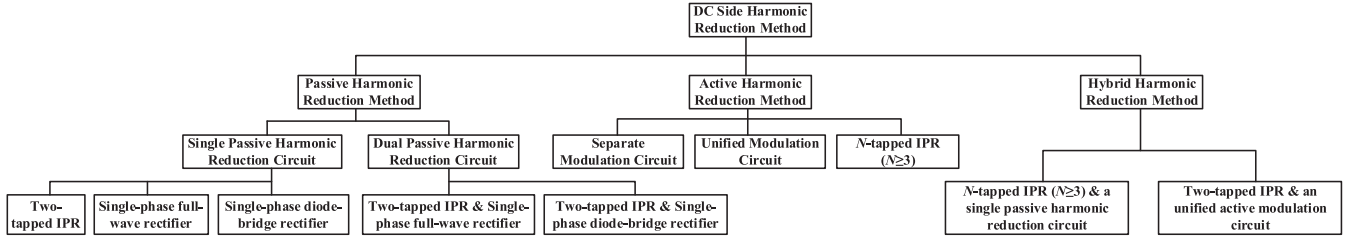


Fig. 1. Classifications for dc-side harmonic reduction methods of MPRs.

is presented in detailed, other simulations and comparisons are not comprehensive. In previous literature reviews, dc-side harmonic reduction methods are rarely mentioned. In addition, some novel dc-side harmonic reduction methods of MPRs with good properties proposed in recent five years [10]–[18], [24], [25], [36], [38]–[40] are not included as well.

This review clarifies and compares some common-used and novel passive, active, as well as hybrid dc-side harmonic reduction methods from a completely new aspect. Fig. 1 shows classifications for dc-side harmonic reduction methods mentioned in this article. Basically, the dc-side harmonic reduction methods can be divided into two kinds, which are the passive harmonic reduction method and the active method. Besides, some research works combine these two methods together to form hybrid harmonic reduction methods, thus this review introduces three kinds of dc-side harmonic reduction methods. Passive harmonic reduction methods are based on passive devices and they have one kind of realization form on each side of IPR. Features for active harmonic reduction circuits are that they include active devices and combine with pulse width modulation (PWM) technology. From Fig. 1, it can be seen that the hybrid harmonic reduction method is a combination of passive and active methods, which contains both passive and active devices. Generally, each kind of method has its own characteristics. Passive methods often have simple structures but harmonic reduction ability is limited; active harmonic reduction methods have better harmonic reduction effects, but control and drive circuits have to be designed, and some active harmonic reduction methods cannot increase pulse numbers. In a dc-side hybrid harmonic reduction circuit, the active part is used for eliminating higher harmonics, which cannot be totally eliminated by passive harmonic reduction circuit; the passive part also has another function to increase pulse number so that improving dc-side output power quality. Therefore, a hybrid harmonic reduction method can give considerations on the power quality of ac and dc sides. Accordingly, it is a useful work to do a comprehensive review of typical harmonic reduction methods, which can provide a fast search and has the potential to provide guidelines for researchers to choose and design suitable dc-side harmonic reduction strategies under various conditions.

In this article, passive and active harmonic reduction mechanisms are analyzed based on two simple circuits in Section II. Sections III and IV, respectively, present comparisons on MPRs with dc-side passive, active, and hybrid harmonic reduction methods, advantages, drawbacks, and utilization occasions are clearly illustrated from aspects that can directly reflect their harmonic reduction abilities, such as total harmonic distortion

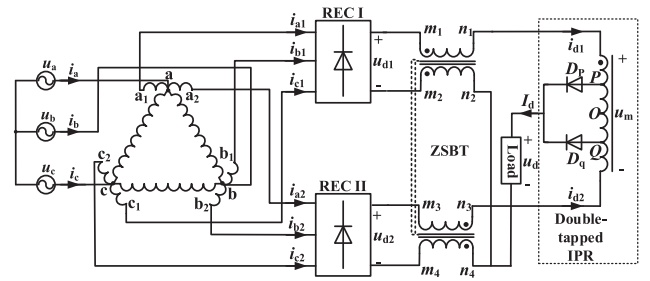


Fig. 2. 24-pulse rectifier with double-tapped IPR.

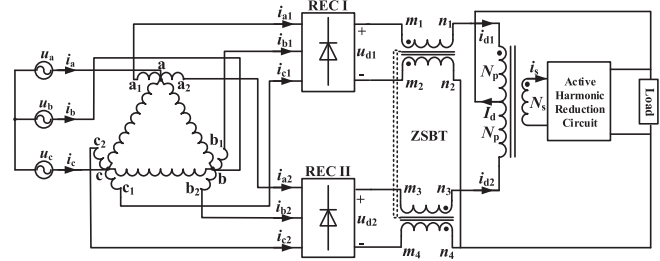


Fig. 3. 12-pulse rectifier with AIPR.

(THD) values of input currents, ripple coefficients of output voltages, kilovoltampere (kVA) rating of magnetic devices, power losses on switches and complexity of control circuits. Besides, some simulations verifications are also presented in Section IV to do further explanations. Finally, the research status and future trends of this topic are summarized in Section VII.

II. HARMONIC REDUCTION MECHANISM ANALYSIS

In this part, the dc-side passive and active harmonic reduction mechanisms are given out based on two kinds of MPRs whose basic circuits are all 12-pulse parallel-connected rectifier. The 24-pulse diode bridge rectifier with double-tapped IPR [6]–[9], as shown in Fig. 2, is taken as an example to illustrate the passive harmonic reduction mechanism. If using an active interphase transformer (AIPR) to replace the IPR in passive harmonic reduction circuits, whose secondary side is connected with an active harmonic reduction circuit [10], a kind of active MPRs is constructed as shown in Fig. 3. The active harmonic reduction circuits could be a single-phase half-bridge converter, single-phase full-bridge converter, or some other circuits that can transfer or absorb the harmonic energy.

Fig. 4 is the winding configuration of the phase-shifting autotransformer used in Figs. 2 and 3. In order to fulfill the

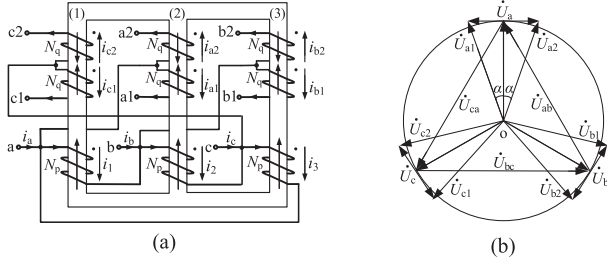


Fig. 4. Winding configuration and phasor diagram of the autotransformer. (a) Winding configuration. (b) Phasor diagram.

phase-shifting requirement of the MPR, the turns ratio $N_p:N_q$ is $\sqrt{3}/(2-\sqrt{3})$. Fig. 4(a) is the winding configuration of the autotransformer shown in Figs. 2 and 3, in which the windings N_p correspond to the three delta-connected windings in Figs. 2 and 3, the windings N_q correspond to the six extended windings in Figs. 2 and 3. The zero-sequence blocking transformer (ZSBT) has high impedance on triple frequency currents to ensure normal conduction of diodes. Both IPR and AIPR all have two main functions, they can absorb instantaneous voltage difference of the two parallel-connected bridge rectifiers to realize their independent operation, and the other function is to generate the needed circulating currents that can counteract harmonics at the ac side. Assume that the load in these two rectifiers are large inductance load, thus the load current I_d can be seen as a constant value. The detailed theoretical derivation is presented as follows.

A. Passive Harmonic Reduction Mechanism Analysis

Assume that input phase voltages of the autotransformer are

$$\begin{cases} u_a = \sqrt{2}U_m \sin \omega t \\ u_b = \sqrt{2}U_m \sin(\omega t - 120^\circ) \\ u_c = \sqrt{2}U_m \sin(\omega t + 120^\circ) \end{cases} \quad (1)$$

where U_m is the rms value of the input phase voltage.

Based on the modulation theory, the output voltages of the two bridge rectifiers (REC I and REC II) are

$$\begin{cases} u_{d1} = S_{a1}u_{a1} + S_{b1}u_{b1} + S_{c1}u_{c1} \\ u_{d2} = S_{a2}u_{a2} + S_{b2}u_{b2} + S_{c2}u_{c2} \end{cases} \quad (2)$$

where u_{a1} , u_{b1} , u_{c1} , u_{a2} , u_{b2} , and u_{c2} are the output phase voltages of the autotransformer, and S_{a1} , S_{b1} , S_{c1} , S_{a2} , S_{b2} , and S_{c2} are the switching functions of each phase.

Relations between each phase current and output currents of the two bridge rectifiers are

$$\begin{bmatrix} i_{a1} \\ i_{b1} \\ i_{c1} \end{bmatrix} = \begin{bmatrix} S_{a1} \\ S_{b1} \\ S_{c1} \end{bmatrix} i_{d1} \quad \begin{bmatrix} i_{a2} \\ i_{b2} \\ i_{c2} \end{bmatrix} = \begin{bmatrix} S_{a2} \\ S_{b2} \\ S_{c2} \end{bmatrix} i_{d2}. \quad (3)$$

S_{a1} can be presented as follows, and the other functions can be derived out based on the conduction mechanism of each diode:

$$S_{a1} = \frac{1}{2} [\text{sgn}(u_{a1} - u_{c1}) - \text{sgn}(u_{b1} - u_{a1})]. \quad (4)$$

Taking phase ‘‘a’’ as an example, based on Fig. 4 and the principle of Ampere-turns balance, the input current i_a can be

expressed as

$$i_a = i_{a1} + i_{a2} + \frac{2 - \sqrt{3}}{\sqrt{3}}(i_{c2} - i_{b2} + i_{b1} - i_{c1}) \quad (5)$$

where i_{a1} , i_{b1} , i_{c1} , i_{a2} , i_{b2} , and i_{c2} are output phase currents of the autotransformer.

In the conventional 12-pulse rectifier, the output current of REC I and REC II is $i_{d1} = i_{d2} = 0.5I_d$. In combination with (3)–(5), the Fourier expansion of ‘‘a’’ phase input current i_{a-12} of the 12-pulse rectifier is

$$i_{a-12} = \frac{6\sqrt{2} - 2\sqrt{6}}{\pi} I_d \left[\sin \omega t - \sum_{k=1}^{\infty} \frac{\sin(12k \pm 1)\omega t}{12k \pm 1} \right] \quad (6)$$

where k is a positive integer.

The dashed portion in Fig. 2 shows the configuration of the double-tapped IPR. O is the mid-point of P and Q , the turns number of PO and OQ are defined as N_{PO} and N_{OQ} , the overall turns number of IPR is N_{all} . According to the voltage relations of u_{d1} and u_{d2} , there are two operation modes of IPR.

The terminal voltage of IPR u_m is equal to the voltage difference of u_{d1} and u_{d2} .

When $u_m < 0$ ($u_{d1} < u_{d2}$), diode D_p is forward-biased and turned on, this operation mode is marked as Mode P. Based on the principle of Ampere-turns balance, Kirchhoff’s current law (KCL) and Kirchhoff’s voltage law, the following relations can be obtained:

$$\begin{cases} (0.5 - \alpha_m)i_{d1} = (0.5 + \alpha_m)i_{d2} \\ u_d = u_{d1} - (0.5 - \alpha_m)(u_{d1} - u_{d2}) \end{cases} \quad (7)$$

where the turns ratio α_m is defined as the ratio of N_{PO} or N_{OQ} to N_{all} .

Mode Q occurs on occasions when $u_m < 0$ ($u_{d1} < u_{d2}$), the diode D_q is turned ON. Under operation Mode Q, the current and voltage relations are presented as follows:

$$\begin{cases} (0.5 + \alpha_m)i_{d1} = (0.5 - \alpha_m)i_{d2} \\ u_d = u_{d1} - (0.5 + \alpha_m)(u_{d1} - u_{d2}). \end{cases} \quad (8)$$

From (7) and (8), after using the double-tapped IPR, i_{d1} , i_{d2} , and u_d are all consisted of two parts, the first part is the same as that values in the conventional 12-pulse rectifier, and the second part is associated with the circulating current generated in IPR

$$\begin{cases} i_{d1} = 0.5I_d + i_m \\ i_{d2} = 0.5I_d - i_m \\ u_d = 0.5(u_{d1} + u_{d2}) + u_{d\alpha}. \end{cases} \quad (9)$$

In (9), the circulating current i_m can be presented as $(S_p - S_q)\alpha_m I_d$, similarly $u_{d\alpha}$ is $(S_p - S_q)\alpha_m(u_{d1} - u_{d2})$. S_p and S_q respectively correspond to switching functions of diode D_p and D_q .

The expression of i_m in the ac side can be obtained based on the KCL, take phase ‘‘a’’ as an example, the influence of i_m on phase ‘‘a’’ can be expressed as:

$$i_{am} = S_{a1}i_m - S_{a2}i_m + \frac{2 - \sqrt{3}}{\sqrt{3}}(S_{b2}i_m - S_{c2}i_m + S_{b1}i_m - S_{c1}i_m). \quad (10)$$

And, the Fourier expansion of i_{am} is

$$i_{am} = \frac{4\sqrt{6}(\sqrt{3}-1)\alpha_m I_d}{\pi} \times \left\{ (\sqrt{6}-\sqrt{2}-1) \left[\sin \omega t + \sum_{k=1}^{\infty} \frac{\sin(24k \pm 1)\omega t}{24k \pm 1} \right] + (\sqrt{6}-\sqrt{2}+1) \left[\sum_{k=1}^{\infty} \frac{\sin(24k-12 \pm 1)\omega t}{24k-12 \pm 1} \right] \right\}. \quad (11)$$

Combining (6) with (11), in the 24-pulse rectifier with double-tapped IPR, the input current of phase ‘‘a’’ is:

$$i_{a-24} = \frac{4\sqrt{6}(\sqrt{3}-1)I_d}{\pi} \times \left\{ \left[\frac{1}{2} + (\sqrt{6}-\sqrt{2}-1)\alpha_m \right] \left[\sin \omega t + \sum_{k=1}^{\infty} \frac{\sin(24k \pm 1)\omega t}{24k \pm 1} \right] + \left[(\sqrt{6}-\sqrt{2}+1)\alpha_m - \frac{1}{2} \right] \left[\sum_{k=1}^{\infty} \frac{\sin(24k-12 \pm 1)\omega t}{24k-12 \pm 1} \right] \right\}. \quad (12)$$

The THD value of i_{a-24} can be expressed by

$$\text{THD}_{i_{a-24}} = \frac{\sqrt{[1+2\alpha_m(-\sqrt{6}-1+\sqrt{2})]^2 \sum_{k=1}^{\infty} \left(\frac{1}{24k-12 \pm 1}\right)^2 + [1+2\alpha_m(\sqrt{6}-1-\sqrt{2})]^2 \sum_{k=1}^{\infty} \left(\frac{1}{24k \pm 1}\right)^2}}{1 + \alpha_m(2\sqrt{6}-2-2\sqrt{2})}. \quad (13)$$

From (13), it is obvious that the turns ratio α_m is associated with the harmonic reduction ability; by doing derivation operation on (13), it can be determined that the optimum value of α_m is $1/2(\sqrt{6}-\sqrt{2}+1)$, and the minimum THD value is about 7.6%.

When substituting α_m into (12), that equation can be rewritten as

$$i_{a-24} = \frac{16\sqrt{3}(2-\sqrt{3})}{\pi(\sqrt{6}-\sqrt{2}+1)} I_d \left[\sin(\omega t) + \sum_{k=1}^{\infty} \frac{\sin(24k \pm 1)\omega t}{24k \pm 1} \right]. \quad (14)$$

From (14), the $(12k \pm 1)$ th (k is an odd number) harmonics can be completely suppressed. For the 24-pulse rectifiers, only $(24k \pm 1)$ th (k is a positive integer) harmonics contain in their input currents. Extend this conclusion to an N -pulse rectifier, the harmonic orders in the input current of an N -pulse rectifier are $(Nk \pm 1)$ th (k is a positive integer). In reality, the harmonic content decreases as the harmonic order increases so that increase of pulse number has impact on harmonic reduction to some extent.

Compared (6) with (11), the harmonic elimination effect of i_{am} can be found. When α_m takes $1/2(\sqrt{6}-\sqrt{2}+1)$, the $(12k \pm 1)$ th (k is an odd number) harmonics in i_{am} has the same amplitude of their corresponding harmonic components in i_{a-12} , but they are opposite in phase. Thus, these order harmonics are disappeared in i_{a-24} . However, in a specific rectification system,

the optimum value of α_m is constant, which makes a passive harmonic reduction circuit only has limited harmonic reduction ability. Compared to the conventional 12-pulse rectifier, although the input current THD of the 24-pulse rectifier has been reduced from 15.2% to 7.6%, it still has $(12k \pm 1)$ th (k is an even number) harmonics. It is necessary to use an active harmonic reduction method to do further harmonic reduction.

This part is mainly focused on the influence of the ac-side input current, so the related content of dc-side voltage is only a brief description. Defining the load voltage ripple coefficient satisfies

$$K = \frac{(u_{d\max} - u_{d\min})}{2u_{d\text{av}}} \quad (15)$$

where $u_{d\max}$, $u_{d\min}$, and $u_{d\text{av}}$ are the maximum value, minimum value, and average value of the load voltage respectively.

From (7)–(9), the circulating currents generated by the alternative conduction of diodes (D_p and D_q) in two taps can produce additional voltages on the load to reduce its ripple coefficient, which can be verified by theoretical calculations through (15). In the 24-pulse rectifier, the load voltage ripple coefficient K reduces from 1.720×10^{-2} in the conventional 12-pulse rectifier to 4.096×10^{-3} under the optimum design. It is worth noting that the optimum turns ratio α_m takes the same value from perspectives of input current THD or voltage coefficient minimization.

B. Active Harmonic Reduction Mechanism Analysis

After using the active harmonic reduction circuit at the secondary side of AIPR, the circulating current flowing through the primary side of AIPR can indirectly modulate the input current to a standard sine wave by shaping the output currents i_{d1} and i_{d2} of the two three-phase diode bridges. In general, the control of the circulating current often reflects on the control of the current i_s which flows into the active harmonic reduction circuit so that it is a key point to determine the shape of i_s when i_a is a pure sine wave.

Based on Fig. 3 and the principle of Ampere-turns balance, the current relations between both sides of AIPR can be obtained

$$(i_{d1} - i_{d2})N_p = i_s N_s \quad (16)$$

where N_p is half the turns number of the primary side winding of AIPR, and N_s is the turns number of the secondary-side winding of AIPR.

In combination with $i_{d1} + i_{d2} = I_d$, expressions of i_{d1} and i_{d2} are

$$\begin{cases} i_{d1} = 0.5(I_d + \frac{N_s}{N_p} i_s) \\ i_{d2} = 0.5(I_d - \frac{N_s}{N_p} i_s). \end{cases} \quad (17)$$

Substitute (3) and (17) into (5), the current i_s can be determined

$$i_s = \frac{i_a - 0.5I_d(S_{a1} + S_{a2}) - \frac{2-\sqrt{3}}{\sqrt{3}} 0.5I_d(S_{b1} - S_{b2} - S_{c1} + S_{c2})}{0.5 \frac{N_s}{N_p} (S_{a1} - S_{a2}) + \frac{2-\sqrt{3}}{\sqrt{3}} 0.5 \frac{N_s}{N_p} (S_{b1} + S_{b2} - S_{c1} - S_{c2})}. \quad (18)$$

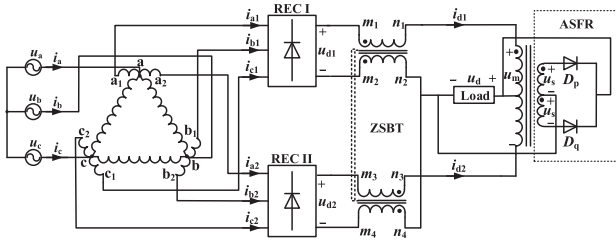


Fig. 5. 24-pulse rectifier with a single-phase full-wave rectifier.

Assume that i_a is a pure sine wave, it can be written as $i_a = \sqrt{2}I_a \sin(\omega t)$, quantitative relations between I_a and I_d can be obtained based on power conservation equation $U_a I_a = U_d I_d$, and in this equation, U_a and U_d have typical relations for a specific topology. Therefore, the shape of i_s/I_d can be draw out, it could be a triangle wave with six times of grid frequency. Through effective control and suitable turns ratio design of AIPR, the needed i_s can be obtained to realize low harmonic input current. Some relative examples are shown in Part IV.

From Fig. 3, it is obvious that the load voltage is still equal to $0.5(u_{d1} + u_{d2})$, which is the same as the conventional 12-pulse rectifier, so this method cannot increase pulse number and without functions for output voltage ripple reduction.

III. DC-SIDE PASSIVE HARMONIC REDUCTION METHODS

One of the typical features of passive harmonic reduction methods is that they are all consisted of passive devices, so passive harmonic reduction methods do not need any additional control or drive circuits. Based on the number of the passive circuits, this method can be divided into the single passive harmonic reduction method and the dual passive harmonic reduction method.

A. MPRs With Single Passive Harmonic Reduction Circuit

In this method, the harmonic reduction circuits are often connected to the secondary side of IPR. In general, the passive auxiliary circuit is a single-phase full-wave rectifier (see Fig. 5) [6] or a single-phase diode-bridge rectifier (see Fig. 6) [7]–[9], whose harmonic reduction mechanism is similar to the method based on multitapped IPRs. The alternative conduction of the diodes in the auxiliary circuit can generate circulating currents to modulate input currents of the rectification system and superimpose additional voltages on the original dc-side load voltage.

All rectifiers showed in Figs. 2, 5, and 6 are 24-pulse rectifiers; there are 24 steps in their input currents and 24 pulses in the load voltage waveforms. The theoretical THD of 24-pulse rectifiers is around 7.5%, and the THD values in experiments could be slightly lower than theoretical calculations. This is due to that the leakage inductances in the phase-shifting transformer and other magnetic devices, with a certain filtering effect, cannot be ignored in experiments. For the rectifier with double-tapped IPR, there are no zero intervals in the output currents (i_{d1} and i_{d2}) of the three-phase bridge rectifiers, which may cause commutation overlap. The communication overlap angle could be effectively reduced after using the topologies shown in this section, which

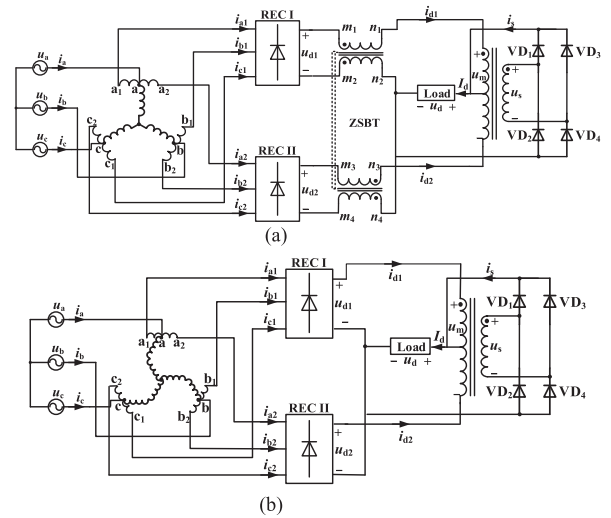


Fig. 6. 24-pulse rectifier with a single-phase diode-bridge rectifier. (a) 24-pulse rectifier with a star-connected autotransformer. (b) 24-pulse rectifier with a zigzag autotransformer.

can add a zero-interval to i_{d1} and i_{d2} . In addition, the auxiliary circuit is installed to cross the load, which provides a feedback loop of the power consumed by the load and, thus, reduce the total power consumption.

In rectification systems, transformers as a kind of high-capacity magnetic device often have an essential influence on the total kVA rating of magnetic devices. Although rectifiers based on isolated transformers have inherent ability to prevent zero-sequence components and avoid using ZSBT, transformer's kVA rating is quite higher, which could be over than load power in most cases. However, the kVA rating of some kinds of autotransformers is lower than isolated transformers, such as the delta-connected (see Fig. 5), the star-connected [see Fig. 6(a)], and the zigzag configured [see Fig. 6(b)] autotransformers only take around 26%–29% of the load power. Although delta or star-connected autotransformers need to be cooperatively used with ZSBT or other devices to prevent zero-sequence components, the kVA rating of ZSBT is only about 10% of the load power. Therefore, in comparison with the isolated transformer, the use of autotransformers can highly reduce the volume, total cost, and power losses of the system to provide the same load power. The 24-pulse rectifier shown in Fig. 6(b) contains a zigzag configured transformer that can expel ZSBT, thus further reducing the total kVA rating of the magnetic devices. In some cases where electric isolation is not required, autotransformers are economical choices to improve power density.

If only one passive harmonic reduction circuit is used at the dc side of a parallel-connected 12-pulse rectifier, only 24-pulse rectifiers can be formed, but this method is easy to combine with other passive or active methods for better performances.

B. MPRs With Dual Passive Harmonic Reduction Circuits

A dual passive harmonic reduction method is a combination of the above-mentioned single passive harmonic reduction methods. In general, the primary side of the IPR installs two taps, and the single-phase full-wave rectifier or single-phase diode-bridge

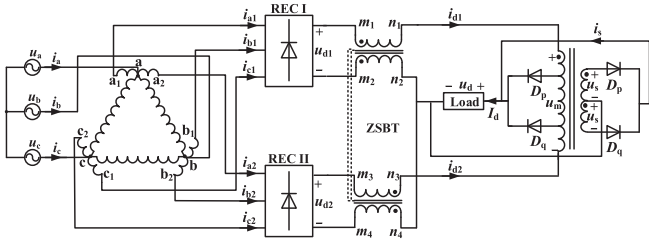


Fig. 7. 36-pulse rectifier with double-tapped IPR and single-phase full-wave rectifier.

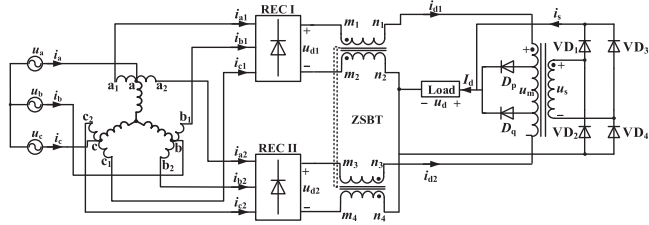


Fig. 8. 36-pulse rectifier with double-tapped IPR and single-phase diode-bridge rectifier.

rectifier is installed at the secondary side of the IPR, which can work together to increase the pulse number of the MPR.

Figs. 7 and 8 are two kinds of 36-pulse rectifiers with dual passive harmonic reduction circuits at the dc side [15]–[18]. Their IPRs have two taps in the primary side and a secondary side winding that are connected with a single-phase full-wave rectifier, as shown in Fig. 7, and a single-phase diode-bridge rectifier in Fig. 8. Based on voltage relations between IPR and load, there are six operation modes under normal conditions to generate an input current with 36 steps, and the output voltage has 36 pulses. If the circuit connected to the secondary side of IPR is failed, the rectifier can operate in a 24-pulse rectification state, which increases the robustness of the whole rectification system. One of the key points in this design is to determine the tap ratio and turns ratio of the IPR, which can be calculated from the perspective of minimizing the THD of the input line current. Under the optimum design, the theoretical THD value of the input current is around 5%, which may have a slight fluctuation in reality due to leakage inductance variations in magnetic devices. Some experiments are carried out to verify the adaptability of the rectifiers, the results indicate that the THD value only has small fluctuations under resistive load variations, which fulfills power quality requirements in most applications.

Although the kVA rating of the multiwinding IPR is slightly higher than the single winding IPR, it is still at a low level, accounting for only about 3% of the load power. The kVA rating of the phase-shifting transformer is roughly the same as described in Section III-A. Besides, only uncontrolled devices are used in these rectifiers, the operation modes of the auxiliary circuits are dependent on their own circuit features. Therefore, this harmonic reduction method is easy to realize and the cost is quite low.

As mentioned before, dual passive harmonic reduction methods provide a useful way to improve power quality both on ac

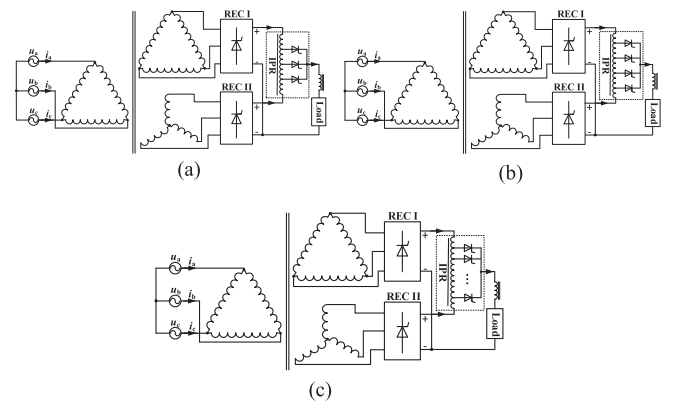


Fig. 9. MPR with controllable tap changer. (a) 36-pulse rectifier with three-tapped IPR. (b) 48-pulse rectifier with four-tapped IPR. (c) MPR with n -tapped IPR.

and dc sides, whose structures are simple and easy to realize. Their implementation only depends on the reconstruction of dc-side modulation circuits in a conventional MPR, without increasing the design complexity of phase-shifting transformers. However, power quality can further be improved by active or hybrid harmonic reduction methods.

IV. DC-SIDE ACTIVE HARMONIC REDUCTION METHODS

Although passive harmonic reduction methods can eliminate some typical order harmonics, some higher order harmonics still exist. In order to obtain a standard sinusoidal input current without harmonic pollutions, the dc-side active harmonic reduction circuits are designed. Based on current relationships between ac and dc links, active harmonic reduction circuits can generate the needed current to modulate the output current of the bridge rectifiers; these output currents can be changed into the form of zero harmonic conditions. According to the modulation characteristics of the active auxiliary circuits, it can be divided into three kinds, the first one is rectifiers based on tap-changer technology, the other two are separate modulation methods and uniform modulation methods. This section still takes the parallel-connected rectifier as a research object to study some typical dc-side active harmonic reduction methods.

A. MPRs Based on Tap-Changer Technology

Replacing the conventional IPR by a double-tapped IPR is an effective way to improve the harmonic reduction performance of the MPR, as shown in Fig. 2. In order to continuously improve the harmonic reduction ability of the MPR, the controllable tap-changer has been proposed to multiply the pulse number [19]–[21].

The topology shown in Fig. 9(a) is a 36-pulse rectifier; the three-tapped IPR are connected with three thyristors, control and drive circuits are needed to control the turn-ON and turn-OFF states of these three switches. Finally, the circulating currents can be formed to eliminate some lower order harmonics and the THD value of the 36-pulse rectifier is about 5.09%. Fig. 9(b) presents the 48-pulse rectifier with a four-tapped IPR, whose theoretical

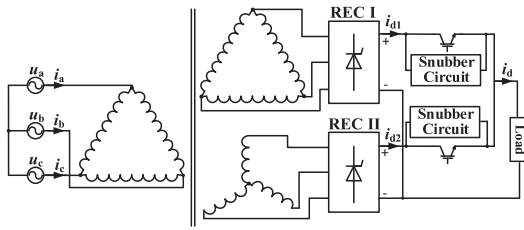


Fig. 10. 12-pulse rectifier with dc-side IGBT modulation circuits.

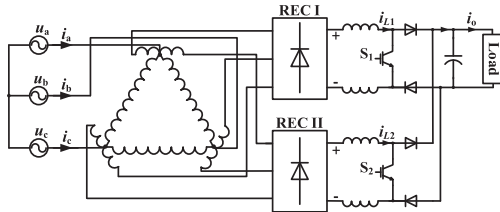


Fig. 11. 12-pulse rectifier with dc-side boost converters.

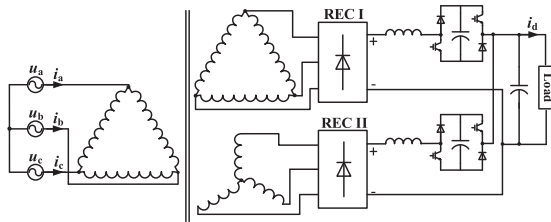


Fig. 12. 12-pulse rectifier with dc-side PWM modulation circuits.

THD is reduced to 3.08%. This method can be extended to a general topology with an n -tapped ($n \geq 3$) IPR, as shown in Fig. 9(c), whose pulse number can be successfully improved to $12n$ as the tap number increases, but the complexity of the control system is correspondingly increased, resulting in higher cost and lower reliability. Moreover, the harmonic reduction ability cannot be maintained in an obviously improved state, that is, the reducing rate of the THD value declines as the increases of the tap number. This is due to that the circulating current produced by this method increases the higher order harmonic content while eliminating lower order harmonics. In this method, the switches on the taps are connected in series with the load; as a result, the conduction losses are quite high.

B. 12-Pulse Rectifiers With DC-Side Separate Modulation Circuits

The dc-side separate modulation method of the multipulse rectification system realizes modulations on the output current of the bridge rectifiers by separately installing an auxiliary circuit on the output side of each rectifier bridge, thereby effectively suppress the input current harmonics of the ac side. Figs. 10–15 depict some rectifiers with different active harmonic reduction methods, and all of them do not require IPRs.

Fig. 10 is an isolated 12-pulse rectifier with the dc-side IGBT modulation circuit, whose current control method is the hysteresis control method [22]. The output currents of the two sets of rectifier bridges are modulated by the turn-on and turn-off of

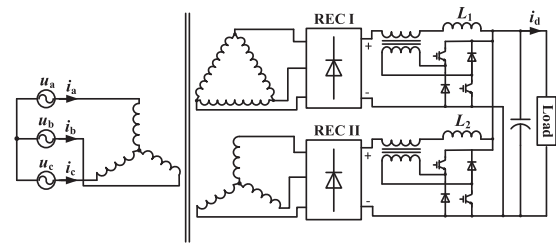


Fig. 13. 12-pulse rectifier with dc-side single-phase inverters.

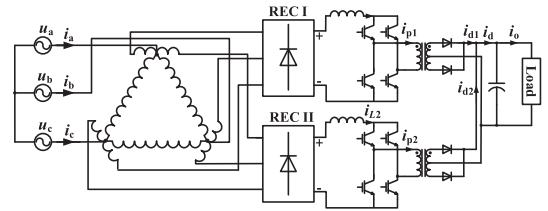


Fig. 14. 12-pulse rectifier with dc-side full-bridge converters.

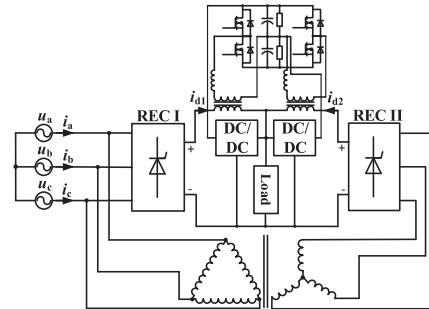


Fig. 15. 12-pulse rectifier with dc-side LSTATCOM circuits.

the IGBT. When the IGBT is turned OFF, current flows through the snubber circuit which is connected in parallel with IGBT. If the modulated output currents of the bridge rectifiers are triangle waves with six times of the grid frequency, the input currents are sine waves, and the THD value is lower than 1% under resistive, small inductive or capacitive load conditions. This circuit has advantages of remarkable harmonic reduction capability, simple structure, convenient control circuit, and good dynamic characteristics. However, the IGBT is connected in series with the main circuit, which increases the switching losses and, thus, limits its applications in high-power industrial occasions.

Fig. 11 presents a 12-pulse rectifier system with dc-side boost circuits [23]–[25]. In this rectifier, the boost circuits are operating under the current continuous mode by properly controlling the currents flowing through the inductors, an approximately sinusoidal input current can be obtained, and the input current THD can be controlled to around 3%. Besides, this circuit has modulation effects on the dc-side output voltage, and the inherent voltage rise characteristic of the Boost converter makes it suitable for high-voltage occasions. Although the IPR can be omitted, two sets of boost circuits directly connected to the main circuit increases power losses when the dc load current is high.

In Fig. 12, the PWM converters are connected at the dc side and controlled by the hysteresis current control method with fast dynamic response [26]. Through reliable control of auxiliary PWM converters, output currents of three-phase rectifiers are critical continuous triangular waves, and then an approximate sinusoidal input current can be obtained based on the current relationship of both sides. In the PWM modulation circuit, switching devices only deal with the ripple voltages, thus the voltage across it is about 10% of the load voltage, the power level of the circuit is quite low, low-power IGBT or MOSFET can satisfy the conditions. Besides, the balanced reactor is omitted, which is beneficial to increase the power density of the system. However, the switching device is directly connected in series with the main circuit, the current is high and the loss is large, which limits utilization in high current and high power occasions.

The following three methods, as shown in Figs. 13–15, all use transformers to connect the main circuit and the active harmonic reduction circuits.

The active harmonic reduction circuits in Fig. 13 are two sets of the single-phase voltage source inverter, which are coupled outside the load current loop by small-capacity single-phase transformers [27]. By properly designing the turns ratio of the single-phase transformer, the current level of the auxiliary circuit can be effectively reduced. Therefore, the problem of large switching losses in the PWM converter directly connected in series with the main circuit can be avoided (see Fig. 12). If the inverter is controlled to generate a specific ac auxiliary voltage, the voltage waveforms on output-side inductors of the two sets rectifier bridges can be changed accordingly so that the output currents of the rectifier bridges can achieve the required current value, and finally, the suppression of the grid side harmonics is realized. This method has advantages of good harmonic reduction effect, low auxiliary circuit power level, and low switching losses, which is suitable for middle- or high-power occasions, but it has two additional inverters and transformers, which needs complex control circuit to obtain high-precision ac-side current phase and amplitude of inverters.

Just like Fig. 11, the circuit presented in Fig. 14 also has power factor correction (PFC) function [28]. Two sets of dc-side full-bridge dc/dc converters are connected in parallel, and they are isolated from the main circuit through isolated transformers. This topology can also provide galvanic isolation for ac and dc sides. If the currents flowing through the inductors fulfill some typical conditions, the output currents of bridge rectifiers are modulated to obtain a sinusoidal input current waveform. But this circuit structure is complex and utilization of so many switches can bring more power losses, so it has limitations in high power applications.

Fig. 15 proposes a 12-pulse rectifier with a load-side compensator (LSTATCOM) [29], [30], which provides compensation currents for the main circuit transmitted by IPRs to eliminate current harmonics. The controller of LSTATCOM can make real-time detection on output voltages of bridge rectifiers and load currents, so this circuit keeps in good harmonic reduction performances when load power varies from 10% to 110% of load power. Besides, this circuit can compensate grid-side voltage fluctuations or unbalance problems. However, this structure

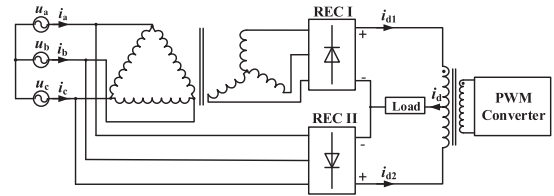


Fig. 16. 12-pulse rectifier with dc-side isolated PWM converter.

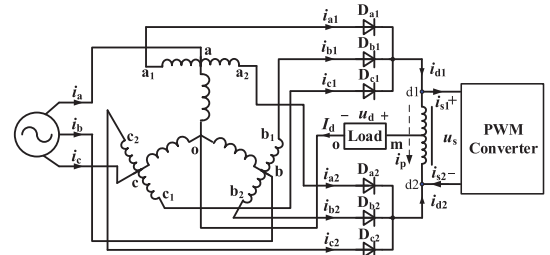


Fig. 17. 6-pulse rectifier with dc-side nonisolated PWM converter.

has so many controls, which is hard to realize in practical occasions.

C. MPRs With DC-Side Unified Modulation Circuits

This section introduces some rectifiers based on dc-side unified modulations, which all need an IPR to provide a common conduction path for modulation currents, input currents are close to sine waves after modulations.

Fig. 16 is a 12-pulse rectifier with a dc-side PWM converter [31] and it is an example of a general mechanism derivation circuit shown in Fig. 3; they have similar circuit configurations and realization forms. It is indicated that, under reasonable control of the PWM converter, this rectifier can present out good harmonic reduction performances, whose ac-side THD_i reduces to 1% under large inductive load conditions. In this delta-wye connected transformer, a set of secondary-side windings is directly connected to the delta-connected windings on the primary side, although it cannot provide entire electric isolation between both sides, the kVA rating of this transformer can be effectively reduced compared to a full isolated transformer. Besides, the PWM converter takes around 3% of load power, so its harmonic reduction cost is quite low, and this method has been widely used in many kinds of main circuits[32]–[35].

Fig. 17 presents a novel structure that can avoid using the secondary side of AIPR [36], so the PWM converter is directly connected with its primary side to reduce the total kVA rating of magnetic devices. It has comparable harmonic elimination mechanisms and effects as the PWM converter connected to the secondary side of AIPR, so its control and drive circuits are also easy to be designed. However, when the dc-side harmonic reduction circuit is out of work, this rectifier could only operate under a 6-pulse rectification state with extremely declined harmonic reduction ability. Therefore, this method can be combined with 12-pulse rectifiers to acquire better power quality.

Fig. 18(a) is a 12-pulse rectifier with a dc-side single-phase boost PFC circuit that contains a single-phase diode bridge

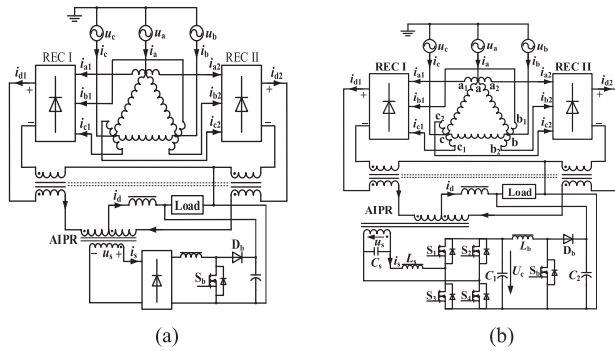


Fig. 18. 12-pulse rectifiers with dc-side single-phase boost PFC scheme. (a) Method with one controllable stage. (b) Method with two controllable stages.

rectifier and a boost converter [37], [38]. This active harmonic reduction method only has a single-stage controllable circuit with advantages of simple structure, easy control, and fast dynamic response so that it can timely modulate operation states of IGBT to obtain needed current i_s under a certain range of circuit parameter variations. However, this PFC circuit only has a function to do current modulations but without any voltage controls due to that its output side is connected in parallel with the load and load voltage is constant, and its front stage is a diode bridge rectifier which has fixed voltage relations between ac and dc sides.

In high-power occasions, if PWM converters are connected in parallel with the load, switches may suffer from high voltage or high current, which increases difficulties in device selection. Besides, large variations of input voltage or load current may cause control distortions of i_s . In order to deal with these problems and ensure harmonic reduction performances, a kind of dc-side active harmonic reduction method with two-stage controllable circuits has been proposed, as shown in Fig. 18(b) [39]; a single-phase diode bridge rectifier in Fig. 18(a) is replaced by a PWM converter here so that it has its own current regulation effects, and then boost converter in Fig. 18(b) can be used for doing voltage regulation. Therefore, the output voltage of the PWM converter can be kept in a reasonable range under large variations of input voltage or load current, and current i_s remains inconsistent with the reference wave. This rectifier also has high robustness for power levels from 1 to 500 kW. Another advantage is that both structures in Fig. 18 provide a feedback path for power absorbed by dc-side harmonic reduction circuit to reach loads, which improves the system's power conversion efficiency.

D. Property Evaluations on Separate and Unified Modulation Circuits

In above-mentioned dc-side active harmonic reduction circuits, the current modulation method of each circuit and their own general properties have been described. In order to present a clearer guideline to users for making an informed choice, this section gives comprehensive property evaluations on separate and unified modulation circuits.

1) *Comparisons of Harmonic Reduction Performances*: The harmonic reduction mechanism of MPRs with dc-side active

TABLE I
THD VALUES OF INPUT CURRENTS FOR MPRs WITH DIFFERENT DC-SIDE ACTIVE HARMONIC REDUCTION METHODS

Harmonic Reduction Method	THD Value of Input Currents (Experimental Results)
Fig. 10	around 1% with a firing angle of 0° [22]
Fig. 11	2.7% (using Y-connected autotransformer) [23]
Fig. 12	4.45% (using delta-connected autotransformer) [24],[25]
Fig. 13	close to sinusoidal wave [26]
Fig. 14	3.8% [27]
Fig. 15	2.7% [28]
Fig. 16	close to sinusoidal wave [29],[30]
Fig. 17	around 1% [31]-[35]
Fig. 18 (a)	4% [36]
Fig. 18 (b)	1% (using delta-connected autotransformer) [37]
Fig. 18 (b)	3.1% (using zigzag autotransformer) [38]
Fig. 18 (b)	1.3% [39]

harmonic reduction methods shown in Figs. 10–18 is to modulate output currents of main rectification circuits into needed shapes that can make ac-side three-phase input currents close to sinusoidal waves. Therefore, the goal of the PWM control is to achieve pure sinusoidal input current waves. However, in reality, there are inevitably minor differences in THD values of input currents, which can be influenced by specific circuit structures, such as harmonic reduction circuits, control circuits, and phase-shifting transformers. Besides, some external factors, such as measurement equipment and experimental surroundings, also have impacts on experimental results. Compared with conventional MPRs without dc-side harmonic reduction circuit, all topologies shown in Figs. 10–18 have considerable harmonic reduction ability, which can reduce input currents THD values into a relatively low level. In [22]–[25], [27], [28], and [31]–[39], authors clearly indicate THD values to clarify the effectiveness of the proposed active harmonic reduction method, some articles like [26], [29], and [30] only present near sine input current waveforms but without THD values. Their specific THD values are shown in Table I.

2) *Comparisons of Structures, Switching Losses, and Control Circuits*: Table II gives comparisons of structures, switching losses, control circuits, and suitable occasions for active harmonic reduction methods shown in Figs. 10–18.

If only takes the dc-side active harmonic reduction circuit (AHRC) into consideration and ignores the main circuit differences, structure and switching losses comparisons of each kind dc-side active harmonic reduction circuits are given in Table II. When the same power is transmitted through MPRs, in addition to the total number of switches, the switching losses mainly depend on the connection relationship between the main circuit and circuit part that contains switches in the dc-side AHRC. If the switches are directly connected in series with the main circuit, the output currents of the two three-phase bridge rectifiers totally flow through the switches, which may largely increase total switching losses under several kilohertz PWM switching frequency. If the circuit part which contains switches is isolated from the main circuit through single-phase transformers, the current flowing through the harmonic reduction circuit can be reduced to a quite low level by the reasonable design of turns ratio in single-phase transformers so that the switching losses level is reduced accordingly. Consequently, the

TABLE II
STRUCTURE, SWITCHING LOSSES, AND CONTROL CIRCUITS COMPARISONS FOR DIFFERENT DC-SIDE ACTIVE HARMONIC REDUCTION CIRCUITS

Fig. No.	Components of AHRC	No. of Switches	No. of Passive Components	Connection Relationship with Main Circuit	Switching Losses	Current Control	Voltage Control	Control Circuit Complexity
Fig. 10	two IGBTs and two snubber circuits	2	not given	non-isolated	high	Yes	No	low
Fig. 11	two Boost converters	2	4	non-isolated	high	Yes	Yes	low
Fig. 12	two single-phase PWM inverters	4	4	non-isolated	high	current is indirectly controlled through voltage control		high
Fig. 13	two single-phase isolated transformer and two single-phase PWM inverters	4	4	isolated	low	same as Fig. 12		high
Fig. 14	two full-bridge DC/DC converters	8	4	half-isolated	high	Yes	Yes	high
Fig. 15	two single-phase half-bridge inverters and two Buck-Boost converters	6	2	isolated	low	Yes	Yes	high
Fig. 16	a single-phase PWM inverter	4	0	isolated	low	Yes	No	low
Fig. 17	a single-phase PWM inverter	4	0	non-isolated	high	Yes	No	low
Fig. 18 (a)	a single-phase diode bridge rectifier and a Boost converter	1	5	isolated	low	Yes	No	low
Fig. 18 (b)	a single-phase PWM inverter and a Boost converter	5	1	isolated	low	Yes	Yes	medium

connection relationship between the main circuit and the AHRC has an influence on the power level of MPRs in applications.

In addition to the ac-side power quality and switching losses, comparison of control circuits is another key point to evaluate overall properties for harmonic reduction circuits. The complexity of the control circuit is associated with the number of switches, the number of control variables, and required control accuracy. The power quality of the MPR is in proportion to the reliability of the control circuit, for AHRC with the complex control circuit, although it may have good harmonic reduction ability and load adaptability, in theory, some problems may arise in real utilization. Therefore, it is an essential work to choose suitable and reliable control design based on a practical use for maintaining good harmonic reduction ability of AHRC.

3) *Overall Evaluations:* Table III lists the overall advantages and disadvantages of AHRC shown in Figs. 10–18, which has the potential to become a useful guideline for designers who concentrated on AHRC research.

V. DC-SIDE HYBRID HARMONIC REDUCTION METHODS

As described in theoretical analysis, passive and active methods have their own advantages and drawbacks; in order to give considerations on both sides' power quality, hybrid harmonic reduction methods consisted of active and passive harmonic reduction circuits are proposed.

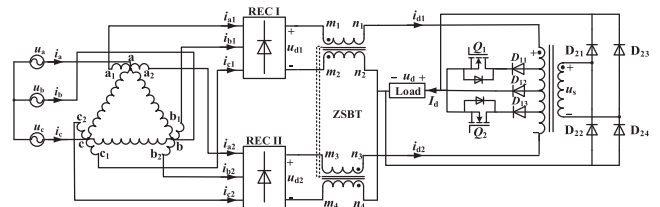


Fig. 19. 48-pulse rectifier with three-tapped IPR and single-phase diode-bridge rectifier.

Based on the dc-side harmonic reduction circuit shown in Fig. 8, the rectifier presented in Fig. 19 increases one tap at the primary side of the IPR; the secondary side of IPR also connects to a single-phase diode-bridge rectifier [40]. Since the primary side of IPR has three taps, controllable devices and their corresponding control circuits are needed. Although this rectification system has increased complexity, it obtains considerable harmonic reduction effects. This rectifier can operate under a 48-pulse rectification state with a reasonable conduction time sequence of switches Q_1 , Q_2 and other power devices, whose theoretical THD_i reduces to around 3.81%. Besides, this 48-pulse rectifier has a quite low kVA rating for IPR which is $2.56\% U_d I_d$.

Actually, this hybrid harmonic reduction method provides a new solution to deal with power quality issues on both ac and dc sides. If we combine one kind of suitable passive and active

TABLE III
OVERALL EVALUATIONS FOR DIFFERENT DC-SIDE ACTIVE HARMONIC REDUCTION CIRCUITS

Fig. No.	Advantages	Drawbacks
Fig. 10	do not need IPR, easy control, good load adaptability	high switching losses, have limitations in high power applications
Fig. 11	do not need IPR, easy control, have a function to modulate output voltage	high switching losses in high power applications
Fig. 12	do not need IPR, low voltage rating of the PWM inverter, high robustness	high switching losses in high power applications, need high control accuracy
Fig. 13	low current level for PWM inverters	need two additional single-phase transformers, need high control accuracy
Fig. 14	provide a galvanic isolation between grid and load, have a function for voltage modulation	control circuit is complex, have limitations in high power applications
Fig. 15	keep good harmonic reduction ability when load variations, have functions to deal with grid voltage unbalance situations	need complex control circuit, hard to realize
Fig. 16	high AC side power quality, low kVA rating of AHRC, easy control	need IPR
Fig. 17	reduced kVA rating of single-phase transformer, easy control	DC side ripple factor is high
Fig. 18 (a)	only one switch, high reliability, easy control	Boost PFC circuit only has current control function
Fig. 18 (b)	high robustness for load variations, effective control circuit design	energy conversion efficiency may be reduced

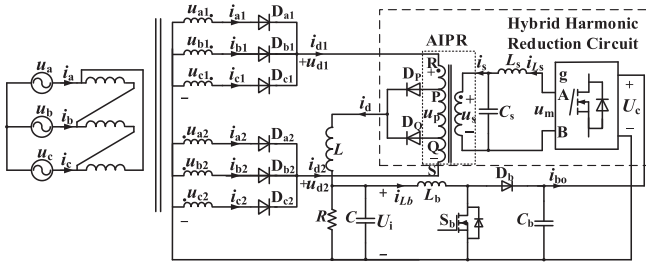


Fig. 20. 12-pulse rectifier with double-tapped IPR and PWM converter.

methods at each side of IPR to construct a novel rectifier, it will have better power qualities on both ac and dc sides.

For example, the harmonic reduction circuit shown in Fig. 20 is a combination of passive and active harmonic reduction circuits respectively shown in Figs. 2 and 18, so it has advantages of these two methods. The active part is used to deal with harmonics that cannot be totally eliminated by a passive harmonic reduction circuit so that the current waveform provided by the active circuit can be designed. Its input current is close to a sine wave under suitable control of current i_s , and the pulse number of load voltage can be doubled compared to its basic circuit.

VI. VERIFICATIONS

In this section, some simulations are carried out based on MATLAB/Simulink to do verifications on performances of some useful and simple dc-side harmonic reduction methods, then doing general comparisons of them. The rms value of three-phase input voltages in simulations is 220 V at the frequency of 50 Hz, and simulation results in Section VI-A are obtained

under a resistive load with a resistance of 30 Ω , while load in Sections VI-B and VI-C is an R - L load (30 Ω , 100 mH).

A. Simulations of Passive Harmonic Reduction Methods

First, the basic model of the parallel-connected 12-pulse rectifier without any harmonic reduction circuit is established. Then the passive harmonic reduction methods presented in Figs. 2, 6(a), 7, and 8 are simulated. Table IV presents some of the main parameters that can indicate their power qualities, such as the THD values of the input current i_a , power factor (PF), and ripple factor (RF) of the load voltage u_{dc} . Figs. 21 and 22 are the input current waveforms, spectrums, and the load voltage waveforms of the rectifiers with 24 pulses [see Fig. 6(a)] and 36 pulses (see Fig. 8).

For uncontrolled rectifiers with a passive harmonic reduction method, the following conclusions can be observed from Table IV and Figs. 21 and 22.

- 1) The input current and output voltage of the N -pulse (N is a positive integer) rectifier, respectively, has an N -step and N -pulse per power supply cycle.
- 2) The input current of the N -pulse rectifier mainly contains the $(Nk \pm 1)$ th (k is a positive integer) harmonics, and the other order harmonics are declined to a quite low level.
- 3) The THD value decreases as the increase of the pulse number, and the specific harmonic reduction circuit or transformer type only has a slight impact on THD variations under the same pulse number.
- 4) The PFs are near to the unit in all simulations, which may have small fluctuations in the experiment.
- 5) The RF of the load voltage also presents a downward trend with of pulse number, whose value is reduced to about 2.3×10^{-3} for the 36-pulse rectifier.

TABLE IV
POWER QUALITY PARAMETERS OF MPRs WITH DC-SIDE PASSIVE HARMONIC REDUCTION METHODS

Pulse No.	Fig. No.	Some Typical Order Harmonics and Contents of Input Current (%) 1th=100%										THD of i_a (%)	PF (%)	RF of u_d
		5th	7th	11th	13th	23rd	25th	35th	37th	47th	49th			
12	/	0.03	0.03	9.41	6.72	4.28	3.62	2.77	2.48	2.05	1.88	14.63	99	1.73×10^{-2}
24	Fig. 2 [6]	0.18	0.09	0.25	0.24	4.47	3.18	0.23	0.23	2.12	1.95	7.04	99	4.28×10^{-3}
	Fig. 6 (a) [7]	0.01	0.01	0.05	0.03	4.47	3.78	0.00	0.00	2.13	1.96	7.29	99	4.73×10^{-3}
36	Fig. 7 [15]	0.09	0.09	0.01	0.01	0.07	0.07	3.30	3.20	0.01	0.01	5.03	99	2.37×10^{-3}
	Fig. 8 [16]	0.15	0.09	0.01	0.01	0.04	0.04	2.89	2.58	0.01	0.01	4.81	99	2.25×10^{-3}

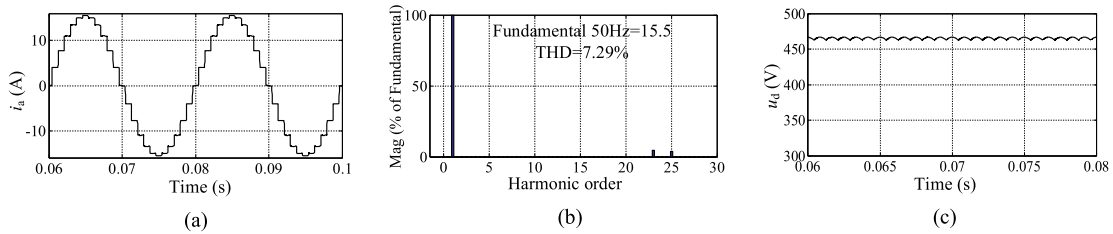


Fig. 21. Input current, spectrum, and load voltage of the 24-pulse rectifier shown in Fig. 6(a). (a) Input current i_{a-24} . (b) Spectrum of i_{a-24} . (c) Load voltage u_{d-24} .

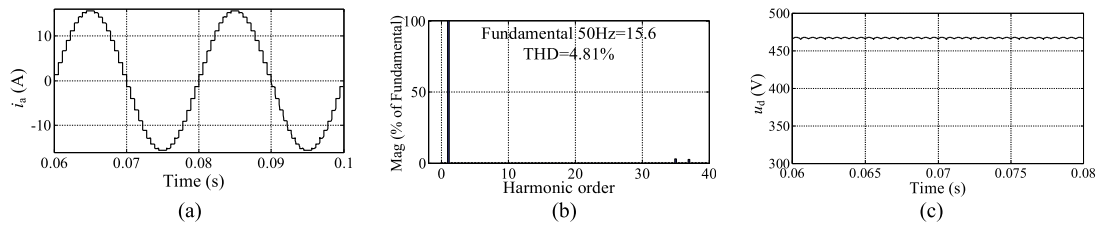


Fig. 22. Input current, spectrum, and load voltage of the 36-pulse rectifier shown in Fig. 8. (a) Input current i_{a-36} . (b) Spectrum of i_{a-36} . (c) Load voltage u_{d-36} .

TABLE V
POWER QUALITY PARAMETERS OF MPRs WITH DC-SIDE ACTIVE HARMONIC REDUCTION METHODS

Pulse No.	Fig. No.	THD of i_a (%)	kVA Rating of Main Magnetic Components and DC Side Harmonic Reduction Circuit (HRC) (% $U_d I_d$)					
			Type of Transformer	kVA Rating of Transformer	ZSBT	AIPR	Type of HRC	kVA Rating of HRC
6	Fig. 17 [36]	3.92	Fork-connected Autotransformer	123	/	10.08	PWM Converter	9.31
	Fig. 11 [23]	2.70	Delta-connected Autotransformer	24.53	/	/	Boost Converters	/
12	Fig. 16 [31]	1.65	Δ/Y Isolated Transformer	57.55	/	4.03	PWM Converter	3.32
	Fig. 18 (a) [37]	3.00	Delta-connected Autotransformer	24.40	7.63	4.71	Boost PFC Circuit	4.72
	Fig. 18 (b) [39]	1.30	Delta-connected Autotransformer	24.70	7.50	3.12	PWM Converter & Boost Converter	2.03

B. Simulations of Active Harmonic Reduction Methods

In this section, the performances of rectifiers presented in Figs. 11 and 16–18 are verified by simulations under conditions of large inductive load. For active harmonic reduction methods, their ac-side power qualities and contents of each order harmonics are not directly related to pulse numbers. So, this part turns to do comparisons of structures and kVA rating of main

magnetic devices (see Table V). In Table V, some parameters are summarized from its original literature; the kVA rating keeps in constant relations with load power for a specific structure, but the THD value might have a fluctuation with variations of load inductance. Figs. 23 and 24 are simulation results of rectifiers shown in Figs. 16 and 17; their load conditions are an $R-L$ load of 30Ω , 100 mH .

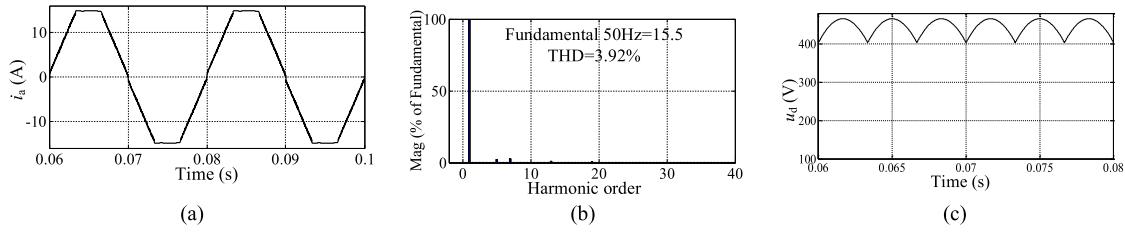


Fig. 23. Input current, spectrum, and load voltage of the 6-pulse rectifier shown in Fig. 17. (a) Input current i_{a-6} . (b) Spectrum of i_{a-6} . (c) Load voltage u_{d-6} .

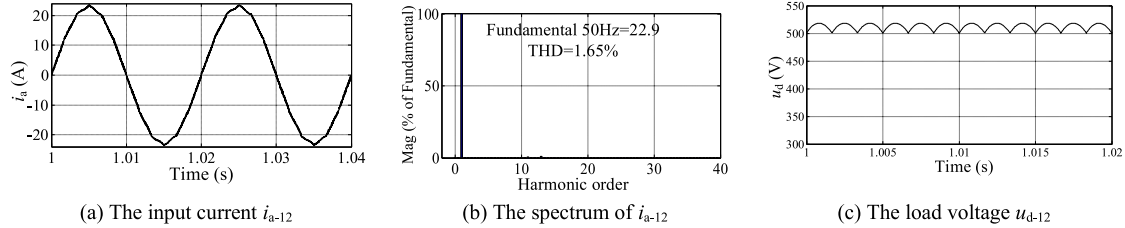


Fig. 24. Input current, spectrum, and load voltage of the 12-pulse rectifier shown in Fig. 16. (a) Input current i_{a-12} . (b) Spectrum of i_{a-12} . (c) Load voltage u_{d-12} .

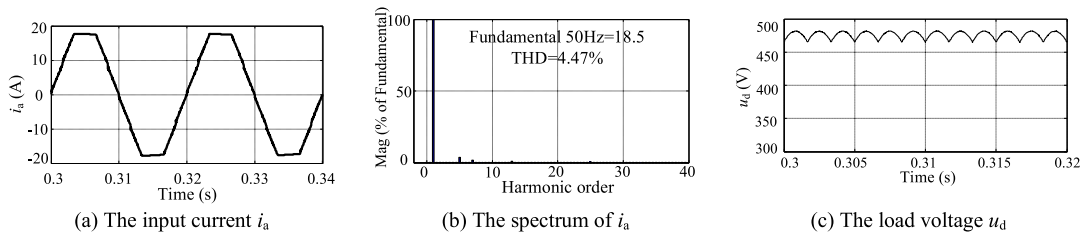


Fig. 25. Input current, spectrum and load voltage of the 12-pulse rectifier shown in Fig. 20. (a) Input current i_a . (b) Spectrum of i_a . (c) Load voltage u_d .

From simulation results, some features of active harmonic reduction circuits can be concluded.

- 1) Although the pulse number of rectifiers in Figs. 11, 16, and 18(a) is 12, THD_i is reduced to less than 3% in simulations, which is much lower than 12-pulse passive rectifiers. The rectifier in Fig. 17 has six pulses but it can also obtain a better input current with THD of 3.92%. They all have considerable harmonic reduction ability.
- 2) The kVA rating of the PWM converter shown in Fig. 17 is about $9.31\%U_dI_d$; an extra power of $4.65\%U_dI_d$ will be added to IPR when using both sides IPR under the same load power. So, this method is helpful for the kVA rating decline of magnetic devices. Other unified modulation circuits could also be directly connected at the primary side of AIPR to reduce its cost and volume.
- 3) For rectifiers with the same pulse number, compared to autotransformers, isolated phase-shifting transformers often need more kVA rating to achieve the same output load power, so autotransformers may be better choices for occasions that do not need isolation on both sides.

C. Simulations of Hybrid Harmonic Reduction Method

Fig. 25 is the simulation results of the 12-pulse rectifier with the dc-side hybrid harmonic reduction method shown in Fig. 20.

Fig. 25(a) is the input current i_a , (b) is the spectrum of i_a , and (c) is the load voltage u_d .

Compared with Fig. 23, although input current THD has a slight fluctuation after adding the passive harmonic reduction circuit, it still at a lower level. The pulse number of the output voltage increases from 6 to 12 so that the passive harmonic reduction circuit has a function for pulse number increasing. If this kind of hybrid harmonic reduction circuit is used in a 12-pulse basic rectifier, better power quality can be achieved.

VII. CONCLUSION AND FUTURE TRENDS

Harmonic reduction mechanisms are foundations of this topic; both passive and active methods are designed based on their own mechanisms, so two examples are selected to illustrate general harmonic reduction mechanisms in Section II. Then some dc-side harmonic reduction circuits with good performances are classified into active, passive, and hybrid methods. Operation principles, functions, and limitations of each method are illustrated in detail; moreover, useful simulation results and comparisons are also given out. This literature review is expected to be a helpful guideline for designers and users to do intensive research or fast searches of MPRs' dc-side harmonic reduction methods under their needed occasions.

The development trend of MPRs is toward high efficiency, enhanced reliability, easy implementation, more economical, and more compact structures with higher input and output power qualities. In order to improve overall performances of MPRs, properly designed dc-side harmonic reduction methods are an important prerequisite. For passive harmonic reduction methods, choosing suitable structures under particular occasions to obtain a higher pulse number is useful for harmonic eliminations. For active harmonic reduction methods, they usually have better harmonic reduction effects than passive methods under the same pulse number, but controllable devices are needed, which increases total costs and design complexities. In addition, it is worth noting that hybrid harmonic reduction methods have potential advantages to give considerations on the power qualities of both ac and dc sides. Therefore, tradeoffs in power quality and other aspects to design more reliable and sustainable harmonic reduction methods of MPRs should become future research orientation.

REFERENCES

- [1] B. Singh, S. Gairola, B. N. Singh, A. Chandra, and K. Al-Haddad, "Multipulse ac-dc converters for improving power quality: A review," *IEEE Trans. Power Electron.*, vol. 23, no. 1, pp. 260–281, Jan. 2008.
- [2] M. H. Rahaman and M. R. Islam Sheikh, "A review of multi-pulse AC-DC power converters," in *Proc. 2nd Int. Conf. Elect. Electron. Eng.*, Rajshahi, Bangladesh, Dec. 2017, pp. 1–4.
- [3] J. Wen, H. Qin, S. Wang, and B. Zhou, "Basic connections and strategies of isolated phase-shifting transformers for multipulse rectifiers: A review," in *Proc. Asia-Pacific Symp. Electromagn. Compat.*, 2012, pp. 105–108.
- [4] A. N. Arvindan and A. Guha, "Novel topologies of 24-pulse rectifier with conventional transformers for phaseshifting," in *Proc. 1st Int. Conf. Elect. Energy Syst.*, Newport Beach, CA, USA, 2011, pp. 108–114.
- [5] S. Prakash P, R. Kalpana, B. Singh, and G. Bhuvaneshwari, "A 20-pulse asymmetric multiphase staggering autoconfigured transformer for power quality improvement," *IEEE Trans. Power Electron.*, vol. 33, no. 2, pp. 917–925, Jan. 2018.
- [6] S. Yang, F. Meng, and W. Yang, "Optimum design of interphase reactor with double-tap changer applied to multipulse diode rectifier," *IEEE Trans. Ind. Electron.*, vol. 57, no. 9, pp. 3022–3029, Sep. 2010.
- [7] L. Gao, F. Meng, and S. Yang, "Harmonic reduction mechanism at DC link of multi-pulse rectifier," *Elect. Mach. Control*, vol. 20, no. 4, pp. 69–77, 2016.
- [8] Q. Pan, W. Ma, D. Liu, Z. Zhao, and M. Jin, "A new critical formula and mathematical model of double-tap interphase reactor in a six-phase tap-changer diode rectifier," *IEEE Trans. Ind. Electron.*, vol. 54, no. 1, pp. 479–485, Feb. 2007.
- [9] S. Choi, B. S. Lee, and P. N. Enjeti, "New 24-pulse diode rectifier systems for utility interface of high-power AC motor drives," *IEEE Trans. Ind. Appl.*, vol. 33, no. 2, pp. 531–541, Mar./Apr. 1997.
- [10] F. Meng, X. Xu, L. Gao, and S. Yang, "Active harmonic elimination in double-star uncontrolled rectifier using active inter-phase reactor," in *Proc. IEEE Veh. Power Propul. Conf.*, 2016, pp. 1–5.
- [11] Y. Lian, S. Yang, K. Xu, Y. Li, and W. Yang, "Harmonic reduction mechanism at DC link of two different 24-pulse rectifiers," in *Proc. IEEE Transp. Electrific. Conf. Expo. Asia-Pacific (ITEC Asia-Pacific)*, Harbin, 2017, pp. 1–6.
- [12] F. Meng, X. Xu, and L. Gao, "A simple harmonic reduction method in multipulse rectifier using passive devices," *IEEE Trans. Ind. Inform.*, vol. 13, no. 5, pp. 2680–2692, Oct. 2017.
- [13] F. Meng, X. Xu, and L. Gao, "A harmonic reduction method in multi-pulse rectifier using passive devices," *Trans. China Electrotech. Soc.*, vol. 32, no. 2, pp. 77–86, Oct. 2017.
- [14] R. Kalpana, K. S. Chethana, S. Prakash P, and B. Singh, "Power quality enhancement using current injection technique in a zigzag configured autotransformer-based 12-pulse rectifier," *IEEE Trans. Ind. Appl.*, vol. 54, no. 5, pp. 5267–5277, Sep./Oct. 2018.
- [15] Y. Li, K. Xu, Y. Lian, W. Yang, and S. Yang, "A novel 36-pulse rectifier with a low loss interphase converter at DC side," in *Proc. IEEE Transp. Electrific. Conf. Expo. Asia-Pacific*, 2017, pp. 2–7.
- [16] S. Prakash P, R. Kalpana, K. S. Chethana, and B. Singh, "A 36-pulse AC-DC converter with DC side tapped interphase bridge rectifier for power quality improvement," in *Proc. IEEE Int. Conf. Power Electron., Drives Energy Syst.*, Chennai, India, 2018, pp. 1–5.
- [17] F. Meng *et al.*, "Dual passive harmonic reduction at DC link of the double-star uncontrolled rectifier," *Trans. Ind. Electron.*, vol. 66, no. 4, pp. 3303–3309, Apr. 2017.
- [18] L. Gao, X. Xu, Z. Man, and J. Lee, "A 36-pulse diode-bridge rectifier using dual passive harmonic reduction methods at DC link," *IEEE Trans. Power Electron.*, vol. 34, no. 2, pp. 1216–1226, Feb. 2019.
- [19] B. Singh, S. Gairola, A. Chandra, and K. Al-Haddad, "Zigzag connected autotransformer based controlled AC-DC converter for pulse multiplication," in *Proc. IEEE Int. Symp. Ind. Electron.*, 2007, pp. 889–894.
- [20] S. Miyairi, S. Iida, K. Nakata, and S. Masukawa, "New method for reducing harmonics involved in input and output of rectifier with interphase transformer," *IEEE Trans. Ind. Appl.*, vol. IA-22, no. 5, pp. 790–797, Sep./Oct. 1986.
- [21] M. E. Villablanca and J. Arrillaga, "Pulse multiplication in parallel converters by multitap control of interphase reactor," *Proc. Inst. Elect. Eng. B, Elect. Power Appl.*, vol. 139, no. 1, pp. 13–20, Jan. 1992.
- [22] M. E. Villablanca, J. I. Nadal, and M. A. Bravo, "A 12-pulse AC-DC rectifier with high-quality input/output waveforms," *IEEE Trans. Power Electron.*, vol. 22, no. 5, pp. 1875–1881, Sep. 2007.
- [23] S. Choi, "A three-phase unity-power-factor diode rectifier," *IEEE Trans. Ind. Electron.*, vol. 52, no. 6, pp. 1711–1714, Dec. 2005.
- [24] F. Meng, J. Luo, L. Gao, W. Yang, and S. Yang, "A high power density multi-pulse rectifier based on harmonic reduction technology at DC link," *Trans. China Electrotech. Soc.*, vol. 32, no. 19, pp. 134–140, Oct. 2017.
- [25] Z. Liu, F. Meng, and W. Yang, "Harmonic reduction technology at DC link in star-connected-autotransformer-based multi-pulse rectifier," in *Proc. IEEE Transp. Electrific. Conf. Expo. Asia-Pacific (ITEC Asia-Pacific)*, Harbin, 2017, pp. 1–6.
- [26] N. R. Raju, A. Daneshpooy, and J. Schwartzberg, "Harmonic cancellation for a twelve-pulse rectifier using DC bus modulation," in *Proc. Conf. Rec. IAS Annu. Meeting*, 2002, pp. 2526–2529.
- [27] P. Chen, X. Li, L. Gong, and Z. Xiong, "A 12-pulse rectifier with an auxiliary circuit," *China Soc. Elect. Eng.*, vol. 26, no. 23, pp. 163–166, Dec. 2006.
- [28] S. Choi and Y. Bae, "A new unity power factor telecom rectifier system by an active waveshaping technique," in *Proc. Conf. Rec. IAS Annu. Meeting*, 2005, pp. 917–922.
- [29] M. Peterson and B. N. Singh, "A novel load compensator for a 12-pulse diode converter," in *Proc. Int. Conf. Power Electron., Drives Energy Syst.*, New Delhi, 2006, pp. 1–6.
- [30] M. Peterson and B. N. Singh, "Multipulse AC-DC thyristor converter with DC bus current shaper," in *Proc. IEEE Power Eng. Soc. Gen. Meeting*, Tampa, FL, 2007, pp. 1–8.
- [31] S. Choi, P. N. Enjeti, H. Lee, and I. J. Pitel, "A new active interphase reactor for 12-pulse rectifiers provides clean power utility interface," *IEEE Trans. Ind. Appl.*, vol. 32, no. 6, pp. 1303–1311, Nov./Dec. 1996.
- [32] B. S. Lee, P. N. Enjeti, and I. J. Pitel, "Optimized active interphase transformer for auto-connected 12-pulse rectifiers results in clean input power," in *Conf. Proc. IEEE Appl. Power Electron. Conf. Expo.*, 1997, vol. 2, pp. 666–671.
- [33] J. Wang, S. Yang, and W. Yang, "Harmonic reduction for 12-pulse four star thyristor rectifier with active auxiliary circuit," in *Proc. Int. Conf. Power Electron. Drive Syst.*, Jun. 2015, pp. 301–306.
- [34] W. Yang, F. Meng, and S. Yang, "Harmonic suppression of multi-pulse AC-DC converter with recycling system of harmonic energy at DC side," in *Conf. Proc. IEEE 7th Int. Power Electron. Motion Control Conf.*, Jun. 2012, pp. 2743–2747.
- [35] A. Kaplon, J. Rolek, and H. Tunia, "The method for reducing harmonics in input currents of rectifier using a modulation in interphase transformer," in *Proc. 5th IEEE Annu. Int. Energy Convers. Congr. Exhib.*, 2013, pp. 117–121.
- [36] F. Meng, X. Xu, L. Gao, and C. Cai, "Active harmonic reduction using DC-side current injection applied in a novel large current rectifier based on fork-connected autotransformer," *IEEE Trans. Ind. Electron.*, vol. 64, no. 7, pp. 5250–5264, Jul. 2017.
- [37] B. S. Lee, J. Hahn, P. N. Enjeti, and I. J. Pitel, "A robust three-phase active power-factor-correction and harmonic reduction scheme for high power," *IEEE Trans. Ind. Electron.*, vol. 46, no. 3, pp. 483–494, Jun. 1999.

- [38] V. Sheelvant, R. Kalpana, and B. Singh, "Improvement in harmonic reduction of zigzag autoconnected transformer based 12-pulse diode bridge rectifier by current injection at dc side," *IEEE Trans. Ind. Appl.*, vol. 53, no. 6, pp. 3634–3644, Nov./Dec. 2017.
- [39] F. Meng, W. Yang, S. Yang, and L. Gao, "Active harmonic reduction for 12-pulse diode bridge rectifier at DC side with two-stage auxiliary circuit," *IEEE Trans. Ind. Inf.*, vol. 11, no. 1, pp. 64–73, Feb. 2015.
- [40] Y. Lian, S. Yang and W. Yang, "Optimum design of 48-pulse rectifier using unconventional interphase reactor," *IEEE Access*, vol. 7, pp. 61240–61250, 2019.
- [41] J. R. Rodríguez *et al.*, "Large current rectifiers: State of the art and future trends," *IEEE Trans. Ind. Electron.*, vol. 52, no. 3, pp. 738–746, Jun. 2005.
- [42] A. C. Lourenço I, F. J. M. Seixas, J. C. Pelicer, and P. S. Oliveira, "18-pulse autotransformer rectifier unit using SEPIC converters for regulated DC-bus and high frequency isolation," in *Proc. IEEE 13th Brazilian Power Electron. Conf. (COBEP/SPEC)*, Fortaleza, 2015, pp. 1–6.
- [43] C. Young, S. Wu, W. Yeh, and C. Yeh, "A DC-side current injection method for improving AC line condition applied in the 18-pulse converter system," *IEEE Trans. Power Electron.*, vol. 29, no. 1, pp. 99–109, Jan. 2014.
- [44] B. Singh *et al.*, "A review of single-phase improved power quality ac-dc converters," *IEEE Trans. Ind. Electron.*, vol. 50, no. 5, pp. 962–981, Oct. 2003.
- [45] B. Singh *et al.*, "A review of three-phase improved power quality ac-dc converters," *IEEE Trans. Ind. Electron.*, vol. 51, no. 3, pp. 641–660, Jun. 2004.



Quanhui Li was born in Shandong, China, in 1996. He received the B.S. and M.S. degrees in electrical engineering in 2018 and 2020, respectively, from the Harbin Institute of Technology, Weihai, China, where he is currently working toward the Ph.D. degree in electrical engineering.

His research interests include multipulse rectifiers and high power rectification.



Taiqi Li was born in Yunnan, China, in 1995. He received the B.S. degree in electrical engineering in 2019 from the Kunming University of Science and Technology, Kunming, China. He is currently working toward the M.S. degree in power electronics and power drives with the Harbin Institute of Technology at Weihai, Harbin, China.

His research interests include power electronic transformers and energy routers.



Qingxiao Du was born in Shandong, China, in 1995. She received the B.S. degree in electrical engineering from the Harbin Institute of Technology, Weihai, China, in 2017, and the M.S. degree in electrical power engineering from the University of Southampton, Southampton, U.K., in 2018. She is currently working toward the Ph.D. degree in electrical engineering with the Harbin Institute of Technology.

Her research interests include the multipulse rectifiers and the power electronic transformers.



Fangang Meng (Member, IEEE) was born in Shandong, China, in 1982. He received the B.S. degree in thermal energy and power engineering and the M.S. and Ph.D. degrees in electrical engineering from the Harbin Institute of Technology, Harbin, China, in 2005, 2007, and 2011, respectively.

Since 2011, he has been working as an Associate Professor with the Harbin Institute of Technology at Weihai. His research interests include harmonic detection, stability analysis of converters, and high power rectification.



Lei Gao was born in Hebei, China, in 1982. She received the B.S., M.S., and Ph.D. degrees in electrical engineering from the Harbin Institute of Technology, Harbin, China, in 2005, 2007, and 2012, respectively.

Since 2012, she has been an Assistant Professor with the Harbin Institute of Technology at Weihai. Her current research interests include power electronics and motor drives.